Volume 19, Number 2, 2026. pp. 223-240

Jordan Journal of Physics

ARTICLE

The Role of Neutron Absorbers in SW Creation with Heavy Water in Nuclear Reactor Core

Seyede N. Hosseinimotlagh[a], **Kavoos Abbasi**[b] , **Mohammad A. Zarei**[c], **Abuzar Shakeri**[a], **Vahid R. Rezaei**[a], **Jahangir Bayat**[a] and **Hamid R. Vanaie**[d]

[a] *Department of Physics, Shi.C., Islamic Azad University, Shiraz, Iran.*

[b] *Department of Physics, College of Sciences, Yasouj University, Yasouj, 75918-74831, Iran.*

[c] *Department of Physics, Payame Noor University, Tehran, Iran.*

[d] *Department of Sciences, Bu.C., Islamic Azad University, Bushehr, Iran.*

DOI: **https://doi.org/10.47011/19.2.9**

Received on: 02/02/2025; *Accepted on: 29/04/2025*

Abstract: This research introduces new parameters and methods for describing soliton wave (SW) propagation and its relationship with the inherent parameters of a nuclear reactor. The study demonstrates that the neutron reaction rate in a purely absorbing medium propagates as a soliton wave. Within the SW, the spatial profiles of the nuclear fission (NF) rate and the atomic density of the neutron absorber (NA) material remain unchanged during burnup wave propagation. The propagation rate of the burnup SW depends on the initial ratio of the nuclear fission rate to the NA density in the medium.

These nonlinear waves are described using neutron flux and atomic density equations that depend on parameters of both time and space in the medium. Burnup SWs in a diffusive medium are investigated in terms of spatial coordinates and the position of the NA within the diffusion region. The transient characteristics are expressed in terms of (i) time of transient (TOT), required to establish a self-sustaining nuclear burning wave, and (ii) the length of transient (LOT), over which this transition develops. The speed associated with the establishment of the transient region is also determined.

In the asymptotic state, the propagation speed of the wave is evaluated, and the width of the power-producing region is quantified using the Full Width at Half Maximum (FWHM). Numerical calculations indicate that the speed of the burnup SW remains constant with the increase of the diffusion coefficient; however, it increases both the diffusion length and the LOT. Furthermore, the ratio of the LOT to the diffusion length does not change. Similarly, increasing the diffusion coefficient increases the TOT, while the ratio of the TOT to the characteristic time remains unchanged.

Keywords: Burn, Soliton, Diffusive, Absorber, Flux.

1. Introduction

In the 19th century, Russell observed waves on the water surface and called them soliton waves (SWs) [1]. These waves continue to move for a long time and keep their original identity. In fact, it is known that these waves remain unchanged in shape and speed along their path. SWs are local waves that are extremely stable and do not change their nature. The solitons are observed in any scales, if the mathematically common property is held by the master equation. This fact is directly linked to the size and model dependence of the two common properties. The nuclear soliton is found in sub-atomic femto-meter scales whose energy is at the order of MeV. This specific scale arises from the effective unit of motion: the nucleon degree of freedom in case of nuclear soliton. For example, the effective unit of motion for the optical

Corresponding Author: A. Shakeri **Email**: Abuzar.Shakeri6845@gmail.com

soliton is the photon. In nuclear physics, it is well known that nuclear motion at energies on the order of MeV is governed by the independent motion of nucleons [2]. A soliton is a wave characterized by both stability and the preservation of its individuality during propagation. Similarly, a nuclear soliton may be interpreted as a special state of nuclear matter exhibiting perfect fluidity. In the context of reaction theory, perfect fluidity may also be associated with inertial behavior. Therefore, if the existence of nuclear solitons is confirmed, they could be linked to important physical phenomena.

Furthermore, the state of perfect fluidity implies the conservation of vorticity. Since celestial bodies contain large amounts of nuclear matter, a quantitative understanding of nuclear solitons may provide new insights into matter and heat transport processes within compact stars. Perfect fluidity is associated with the dissipation property of low-energy heavy-ion collisions that has been a long-standing open problem in microscopic nuclear reaction theory [3].

To verify the existence of solitons in subatomic quantum systems, we focus on the Korteweg-de-Vries (KdV) equation. This equation is both a nonlinear evolution equation and a dispersive wave equation. Solitary waves that preserve their shape and propagation speed after collisions are referred to as solitons [4]. For an initially given sinusoidal wave profile, the wave can split into several solitary waves. These solitary waves exhibit the following characteristic properties: (i) they propagate stably while preserving their momentum and shape, even after collisions; and (ii) they may experience phase shifts and time delays during collisions. These features are regarded as the defining properties of soliton waves (SWs) [5]. That is, the solitary wave is called a soliton if it possesses the above features. The transparency associated with the preservation of individuality is often referred to as the particle-like property in soliton theory. In particular, comparisons of SWs before and after collisions show that their momentum and shape remain unchanged, although phase shifts may occur.

Nonlinear partial differential equations have a considerable influence on the study of nonlinear physical sciences. These equations are often used to elucidate many intricate natural phenomena. Nonlinear partial differential equations are mainly used to characterize the behaviors of waves in the form of solitons and solitary waves. As a result, the investigation of nonlinear waves plays a substantial role in our daily lives and in a variety of research fields, including hydrodynamics, fluid dynamics and mechanics, earth science, solid-state physics, water waves, chaos theory, and quantum mechanics, among others. These expanded models have encouraged a multitude of potential research projects and significantly elucidated the physical properties of engineering and physics applications. Consequently, the study of nonlinear partial differential equations has consistently attracted considerable interest in recent years. Nonlinear differential equations represent various scientific experimental models. To comprehend the intrinsic characteristics of the nonlinear model, finding analytical and accurate solutions to the models is essential. It is necessary to investigate the solutions and characteristics of nonlinear partial differential equations in order to understand the structure they represent. Researchers have developed a number of efficient methods using symbolic computations to ensure the accuracy of soliton solutions to nonlinear partial differential equations. Numerous problem-solving methods have their own advantages and requirements when used in management models. Nonlinear partial differential equations are now widely recognized as the most comprehensive way for defining the physical significance of nonlinear scenarios occurring in the fields of science and engineering.

Numerous studies have demonstrated the characteristics of soliton solutions and their applications in various scientific and technological domains. Soliton theory is a significant field of research in the fields of applied mathematics and mathematical physics. Solitons are wave bundles that are self-sustaining and maintain their shape while traveling at a constant speed, as defined by mathematics and physics. There are numerous varieties of solitons, including dark, bright, peakons, anti-kink, kink, temporal, spatiotemporal, spatial, and singular. Numerous investigations have demonstrated the diverse characteristics of soliton solutions and their applications in scientific and technological fields. Numerous disciplines, such as fluid dynamics, plasma physics, nonlinear optics, coastal engineering, and communications engineering, have significant uses for soliton solutions. They are essential for the advancement of global communication. Advanced analytical and numerical strategies have been devised by mathematicians to ascertain the soliton solutions of various nonlinear partial differential equations. SWs are gaining significance in a variety of fields, such as nonlinear optics, optical fibers, and ferromagnetic materials. This multidisciplinary approach, which integrates mathematics, computer science, and physics, demonstrates the dynamic nature of scientific research when it is applied to real-world issues. By acquiring a more thorough comprehension of SWs, advancements may be made in these fields and novel applications identified. Equations that admit soliton solutions are referred to as soliton equations, and the Korteweg–de Vries (KdV) equation is one of the best-known examples. The KdV equation contains nonlinear terms that describe the propagation of small-amplitude soliton waves (SWs) in dispersive media [2]. Moreover, this equation provides a general framework for studying weakly nonlinear waves in dispersive media. The easiest form of this equation is: $u_t + auu_x + u_{xxx} = 0$, where u_t represents the evolution of wave propagation with time in the x dimension. In addition, the KdV equation contains two important components: (i) the nonlinear term, represented by uu_x, which governs the steepening of the soliton wave (SW); and (ii) the dispersive term, represented by u_{xxx}, which describes wave dispersion during propagation. Nonlinearity tends to localize the wave, whereas dispersion causes it to spread. Studies have shown that in a number of non-linear environments, for example in shallow water, the wave packet broadening caused by scattering can be balanced by the effects of narrowing caused by the non-linear environment. The balance describes the formulation of solitons .The stability of SWs results from the balance between nonlinear and dispersive effects. This equation yields soliton resonators that characterize SWs with particle identities that decay at long distances.

In 1965, researchers numerically investigated the nonlinear interaction between a large soliton wave and a smaller overtaken SW [3]. Their results demonstrated that SWs governed by the KdV equation preserve their identities during nonlinear interactions. The particle-like behavior of SWs, together with their ability to maintain their shape and propagation characteristics after collisions, motivated further investigations into soliton dynamics [3].

The interaction between two solitons is characterized by the preservation of their shape, speed, and pulse properties, indicating that soliton collisions are elastic. In 1995, Seifritz reported his research on burnup wave propagation in pure neutron absorbing media (NAM) [4]. He analyzed this problem theoretically and found that the neutron reaction rate in the diffusive medium is similar to that of SWs. Van Dam subsequently continued this line of research [5-7], with some significantly valuable outcomes [8-11]: (i) burnup waves in diffusive media can be realized by placing neutron absorbers in the reflector region, provided that the reactor core and reflector are neutronically coupled, as in high-temperature gas-cooled reactors; (ii) long term control of excess reactivity can be achieved using spherical or cylindrical particles, which provide greater design flexibility in balancing the reactivity loss caused by fuel burnup with the reactivity gain resulting from the depletion of burnable poisons; and (iii) the width of the reaction zone is approximately three times the absorption mean free path.

In the analysis of neutron behavior in nuclear fission reactors, one of the most important parameters is the determination of the nuclear fission (NF) rate within different regions of the reactor core. Accurate evaluation of the NF distribution is essential for predicting reactor power distribution and other parameters related to the safe operation of the reactor [8]. Therefore, in this study, the diffusion equations are solved for the first time in the form of solitary waves in a one-dimensional D_2O diffusive medium, considering slab reactor geometry with different neutron absorbers. The main objective of this work is to investigate the characteristics of burnup SWs using various isotopic neutron absorbers (NAs) such as: Boron (^{10}B), Cadmium (^{113}Cd), Samarium (^{149}Sm), Europium (^{151}Eu), Hafnium (^{177}Hf) and Gadolinium (^{157}Gd), in a heavy-water diffusive medium. The analysis assumes a net input neutron current incident normally on the slab boundary [9, 10].

The remainder of this article is organized as follows. Section 2 presents the physics of SWs using the Korteweg–de Vries (KdV) equation.

Section 3 discusses the properties of the selected neutron absorbers. Section 4 describes the proposed model. Section 5 presents the results and discussion. Finally, the conclusions are given in Section 6.

2. Physics of Soliton

The KdV equation describes the dynamics of both hydrodynamic and lattice systems and represents a fundamental example within a broad class of SW equations. Here, to examine some of the physical properties of solitons, we also consider the sine-Gordon equation:

$$\varphi_{tt} - \varphi_{xx} + sin\varphi = 0 \qquad (1)$$

This equation possesses several classes of solutions. Since x varies from $-\infty$ to $+\infty$, the solution connecting the interval 0 to 2π corresponds to a soliton solution, whereas the solution connecting 2π to 0 corresponds to an anti-soliton solution.

In 1939, the sine-Gordon equation was proposed as a model for crystal defects [11]. Later, during the 1960s, it was also used in studies of elementary particles [12]. These studies investigated soliton and anti-soliton collisions and confirmed the stability-like behavior of such nonlinear wave structures [13]. In addition, researchers introduced the quantity Q, defined as follows:

$$Q = \frac{1}{2\pi}\{\varphi(\infty, t) - \varphi(-\infty, t)\} \qquad (2)$$

Q must be a constant under the boundary conditions governing the selected system. In the 1967s, researchers [14] made a remarkable discovery in the branch of nonlinear optics, namely that the laser light emitted from 2-level lasers obeys the sine-Gordon equation [15]. One important application of the sine-Gordon equation is in the study of Josephson junctions with magnetic flux propagation. A Josephson junction consists of two superconductors separated by a thin insulating layer. Let η_1 and η_2 denote the phases of the Cooper-pair wave functions in the superconducting plates. According to the Josephson current relation: $j = j_0 sin\eta$,

where $\eta = \eta_1 - \eta_2$, the dynamics of η can be described by the sine-Gordon equation. In general, the sine-Gordon equation has many applications in various branches of science and technology. SWs have been widely used in several areas of physics, including biophysics, hydrodynamics, nuclear fission, astrophysics, plasma, nonlinear optics, condensed matter physics [16-22].

3. Properties of Selected Neutron Absorbers

Burnable absorbers (BAs), also known as burnable neutron poisons, are materials inserted into a nuclear reactor core that contain non-fissile nuclei with large neutron-absorption cross sections. The BAs absorb neutrons, decreasing their population significantly over the course of the core's operational cycle. As the BA abundance decreases, so too does the BA's impact on reactivity. BAs provide numerous benefits, including reactivity control for extended fuel cycles, tritium production, and burning of long-lived radionuclides from spent nuclear fuel [23-24]. While BAs can vary widely based on economics, thermal hydraulics, manufacturing, response to radiation damage, and reprocessing/disposal, they maintain a strong negative reactivity worth, which of course decreases by design as they are depleted due to neutron absorption [25].

Burnable absorbers are often used to reduce power peaking in the core, either for a fresh fuel assembly (typically in light water reactors (LWRs)) or locally within a fuel pin or plate (typically in research and test reactors). The negative reactivity of a BA offsets the positive reactivity of fresh fuel. Depletion of fuel is accompanied by depletion (burnout) of the BA material; ideally, the BA will effectively burn out at the same rate as the fuel in such a way that the net reactivity remains constant with time. If the BA burns out too quickly, then a positive reactivity swing later in the operational fuel cycle could exceed the allowable limits for the reactor. If the BA burns out too slowly, then the remaining BA results in a negative reactivity penalty toward the end of the fuel's operational cycle; however, an exact match is not necessary and typically is not feasible. Local spectral effects will affect the relative depletion of the poison and the fuel. When used in this manner, BA materials may be included within the fuel, either as a homogeneous mixture or a coating, but BA rods can also be used to control local power peaking by appropriate placement of rods within a fuel assembly [26-27]. The two approaches are often combined; gadoliniumbearing fuel rods are used to control assembly reactivity in many boiling water reactor (BWR) designs (*vide infra*). Pressurized water reactors (PWRs) also use soluble boron to control total core reactivity, but because the boron is uniformly distributed in the coolant it is not used to control peaking [28]. Further, soluble boron is not considered to be a burnable absorber as reactivity control is managed by reactor operators by reducing boron content with burnup over a fuel cycle.

Since neutron capture in burnable absorbers is typically spectrum-dependent, BAs are sensitive to changes in temperature. ^{10}B, often used as a burnable poison, is a 1/v absorber whereby its neutron absorption cross-section decreases logarithmically with neutron energy. The magnitude of negative reactivity for ^{10}B decreases with increasing temperature as the thermal Maxwellian shifts toward higher energies [29]. This results in net positive reactivity feedback. ^{155}Gd and ^{157}Gd, on the other hand, while 1/v at very low neutron energies, both have significant resonances above 1 eV and can display increasingly negative reactivity coefficients with respect to temperature, depending on the spectrum of the reactor itself. ^{167}Er has a high thermal resonance at 1 eV that results in increased absorption, leading to a negative reactivity coefficient with respect to temperature; hence, boron and gadolinium are also common BA materials in fast reactors; in a fast reactor spectrum both have removal cross sections that decrease with increasing temperature, so both have net positive temperature reactivity coefficients. While a negative reactivity coefficient for a BA would be desirable in a reactor such that neutron capture increases with increasing temperature, the temperature reactivity coefficient of fuel associated with burnable absorbers is designed to always be negative and will more than offset any positive feedback from burnable absorbers. Of course, the magnitude of the temperature reactivity coefficient will always decrease with burnout of the poison materials [30].

BAs are considered fundamentally different from control rods. Control rods in nuclear reactors can be withdrawn from the reactor core during operation and may remain in service for several years or even decades before replacement. BAs are incorporated into the reactor core material to provide long-term reactivity control. Other neutron poisons present in the reactor core that are produced as fission products are also not considered BAs; rather, they are unavoidable byproducts of nuclear fission reactions [31].

Different nuclear reactor types have different operating conditions, coolants, fuel forms, and neutron spectra which may limit the practicality of some BAs.

As noted earlier, the most common BA materials in commercial LWRs are boron and gadolinium. Boron is used in the standard form of B_4C with the natural boron isotopic composition (approximately 19.9% ^{10}B and 80.1% ^{11}B). ^{10}B has a thermal neutron cross-section of about 3850b; in comparison, thermal absorption in ^{11}B is negligible, with a cross-section of approximately 0.005b for thermal neutrons. When absorbing a thermal neutron, ^{10}B emits an alpha particle (^{4}He) resulting in a ^{7}Li daughter nucleus. As both are stable isotopes, neither is a source of decay heat post-shutdown. However, the accumulation of helium can produce internal pressure, challenging the integrity of high-density fuels or build up between the poison and cladding. Further, neutron capture in ^{7}Li results in the production of tritium. Natural gadolinium (see Table 1 for isotopic abundances and cross sections) is another common BA in commercial reactors due to the high neutron absorption cross-section of ^{155}Gd and ^{157}Gd. Their absorption cross-sections are the highest among all stable isotopes. Relative to boron and other BA materials, which are generally considered to be “gray” absorbers, gadolinium behaves like a “black” absorber for neutrons, making it highly effective in compensating for excess reactivity. However, this same property can result in strong local flux depressions if not properly designed. This phenomenon will be discussed in detail in the next section.

Although less commonly used, hafnium-based materials are attractive BA candidates because of their strong neutron absorption capability at energies above the thermal range, a phenomenon known as resonance energy absorption. In addition, their reactivity worth changes gradually under irradiation, making them suitable for long-term reactor control applications. In Hf, when a neutron is absorbed, some natural hafnium isotopes readily transform into another neutron-absorbing isotope. Hafnium metal also exhibits excellent corrosion resistance in hot water owing to the formation of a protective hafnium oxide (HfO_2) passivation layer on its surface. In its unalloyed form, passivated hafnium corrodes in 400 °C steam at a rate of approximately 1.36 $\mu g \cdot cm^{-2} \cdot day^{-1}$, about 1/8th the rate of Zircaloy-2. Without this passivation layer, however, hafnium degrades rapidly due to the diffusion of hydrogen formed by radiolysis of water, resulting in rapid swelling and embrittlement. This hydride-induced swelling and facture of hafnium has led to the abandonment of hafnium as an absorber material under high temperature/fluence conditions (i.e., commercial applications).

Hafnium-based BAs can also be designed using HfO_2. In principle, HfO_2 may serve as an effective BA material. Whereas UO_2 adopts a fluorite crystal structure, HfO_2 can crystallize in monoclinic, tetragonal, or cubic phases. Under high-temperature conditions, such as those encountered in commercial UO_2 fuel where the centerline fuel temperature may exceed 1300 K, HfO_2 can partially substitute uranium to form a UO_2-HfO_2 solid solution [32]. In addition, nuclear fuel surfaces may potentially be coated with a layer of HfO_2 using deposition techniques; however, there is currently no experimental evidence demonstrating its performance under actual reactor operating conditions [33].

Cadmium-based BAs have attractive neutronic properties for use in extended fuel cycles. Cadmium is also an important component of standard silver-indium-cadmium control rods in both research and commercial nuclear reactors. The neutronic properties of Cd-based BAs allow precise control of BA burnout over a wide range of fuel burnup in comparison with boron (slower-burning) or gadolinium (faster-burning) BAs. Further, cadmium's (n,γ) reaction does not result in helium accumulation. Historically, proposed cadmium-based BAs have taken the form of metallic Cd wires or CdO pellet coatings [34-36]. The use of Cd-based BAs, however, presents fabrication and disposal complications due to significant health concerns. Both Cd and CdO are ranked as a health hazard Level 4 according to the National Fire Protection Association.

The europium (^{167}Er) isotope exhibits a strong resonance near $1eV$, leading to enhanced neutron absorption and consequently a negative temperature reactivity coefficient. In fast reactors, B and Gd are are among the most commonly used burnable absorbers. One of the major challenges associated with these isotopes is their separation and enrichment, which can be costly. Samarium possesses six stable isotopes, among which ^{149}Sm constitutes approximately 14% of natural samarium. This isotope is a strong neutron absorber with a large absorption cross section. In this paper, we focus on the aforementioned burnable absorbers and their properties listed in Table 1, where $\sigma_{a,th}$ and $\sigma_{a,fast}$ represent the thermal and fast neutron absorption cross sections at neutron energies of $0.025\ eV$ and $200\ keV$, respectively.

TABLE 1. Features of different suggested burnable absorbers [35].

Name	Symbol	$T_{1/2}$	Percentage of Frequency	$\sigma_{a,th}(barn)$	$\sigma_{a,fast}(barn)$
Boron	^{10}B	Stable	19.9	9.38	1.97
Cadmium	^{113}Cd	$8.0 \times 10^{15} y$	12.2	38	0/31
Samarium	^{149}Sm	Stable	13.8	40150	0.70
Europium	^{151}Eu	$5.0 \times 10^{18} y$	47.8	9185	0.30
Hafnium	^{177}Hf	Stable	18.5	375	0.55
Gadolinium	^{157}Gd	Stable	15.7	252912	0.33

4. Suggested Model

Neutron diffusion theory provides the key to calculating the NF in a nuclear fission reactor. In the operation of fission reactors, neutron energy and spatial distribution are very important. Neutrons encounter different interactions while moving in the system. Today, diffusion theory is widely used in the core of pressurized and boiling water reactors. This theory provides a physically consistent description of nuclear fission. The theoretical geometry adopted in this work is a one-dimensional semi-infinite slab, which is used to obtain the soliton transition and the stationary state in a burning diffusive medium [37-41]. This model highlights the role of the newly introduced quantities in the development of SWs within diffusive media in nuclear fission reactors. If an increase in propagation speed is required, the NA density must be reduced by introducing neutron moderators into the reactor core. The NF distribution and burnup properties of the diffusive medium containing an NA are evaluated using the neutron diffusion equation with the burnup equation.

4.1. Asymptotic and Exact Solution of SW Equations of an Absorbing Medium

The partial differential equations

$$\frac{\partial\phi(x,t)}{\partial x} = -\sigma N(x,t)\phi(x,t)$$

and $\frac{\partial N(x,t)}{\partial t} = -\sigma N(x,t)\phi(x,t)$

describe the neutron flux attenuation and fuel absorption in a one-dimensional medium with a semi-finite planar geometry. In the general solution of these nonlinear and inseparable equations, we focus on the asymptotic solution. The answer to these equations, for ϕ and N and the reaction rate R, gives a constant form after a transition state. One result of this discussion is that the solutions are simply functions of α=x-vt. The independent variable time can be defined in the general derivative of the function f in the Cartesian coordinate system as:

$$\frac{df}{dt} = \frac{df}{dt} + v\frac{df}{dx} = 0.$$

This operation enables us to derive from the above equations the ordinary nonlinear differential equations of the flux and density of the nuclide:

$$\frac{\partial\varphi_{as}(x,t)}{\partial\alpha} + \sigma\varphi_{as}\left(N_0 - \frac{\varphi_{as}}{v}\right) = 0; \frac{\partial N_{as}}{\partial\alpha} + \sigma N_{as}(N_{as} - N_0) = 0.$$

The subscript "as" denotes asymptotic solution.

5. One-Dimensional Solution of Neutron Diffusion Equation in Solitary Wave Form

The neutron diffusion equation is as follows [7]:

$$D\frac{\partial^2\varphi(x,t)}{\partial x^2} - \sigma N(x,t)\varphi(x,t) = \frac{1}{v}\frac{\partial\varphi(x,t)}{\partial t} \quad (3)$$

where $\varphi(x,t), N(x,t), \sigma, D$ and v are NF, density of NA, NA absorption x-section, diffusion constant, and velocity of neutron, respectively. In this work, we have chosen the geometry presented in Fig. 1.

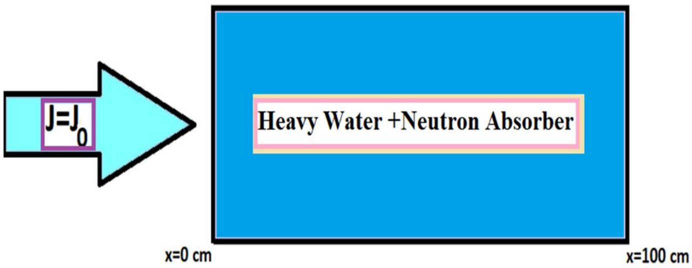

FIG. 1. Schematic illustration of slab neutron diffusion geometry under neutron irradiation in an absorbing medium.

Considering that the temporal variation of the NF rate is very compared with the high neutron speed, the time-derivative term can be neglected. Consquently, the above equation reduces to:

$$D\frac{\partial^2\varphi(x,t)}{\partial x^2} - \sigma N(x,t)\varphi(x,t) = 0 \quad (4)$$

Also, the NA burnup equ. is given by:

$$\frac{\partial N(x,t)}{\partial t} = -\sigma N(x,t)\varphi(x,t) \quad (5)$$

The boundary and initial conditions for selected geometry are:

$N(x,t) = N_{0,}\ \varphi(100,\mathrm{t}) = \varphi_0$

and $J(0,t) = J_0$,

where J is known as current density of neutron. We assume that NF is canceled on the boundary. The rate of reaction is another important parameter, which is given by:

$$R(x,t) = \sigma N(x,t)\varphi(x,t) \quad (6)$$

For each of Equations 4 and 5, an asymptotic solution can be provided, using appropriate boundary conditions:

$$N_{as}(x,t) = \frac{N_0}{\left(1+\exp\left(-\frac{x-vt}{l_0}\right)\right)^{3.5}} \quad (7)$$

$$\varphi_{as}(x,t) = \frac{v\sqrt{2}}{\sigma l_0}\left(\frac{N}{N_0} - 1 - \ln\left(\frac{N}{N_0}\right)\right)^{\frac{1}{2}} \quad (8)$$

and for the asymptotic reaction rate density:

$$R_{as}(x,t) = \frac{v\sqrt{2}}{l_0} N_{as}\left(\frac{N_{as}}{N_0} - 1 - \ln\left(\frac{N_{as}}{N_0}\right)\right)^{\frac{1}{2}} \quad (9)$$

Diffusion length is calculated by: $l_0 = \sqrt{\frac{D}{N_0\sigma}}$. The wave speed is obtained from the relationship $v = \frac{\varphi_0}{N_0}$,. This result can be obtained by considering that the number of fuel-absorbing nuclei consumed per unit time is equal to the number of neutrons entering the medium per unit time:

$$\varphi_0 = -\frac{d}{dt}\int_0^\infty N_{as}(x - vt)dx = -\int_0^\infty \frac{d}{dt} N_{as}(x - vt)dx = \int_0^\infty v\frac{d}{dx} N_{as}(x - vt)dx = vN_0 \quad (10)$$

Now, by using the asymptotic solutions which are described in section 4-1 and by integrating each of equations $\frac{\partial\phi(x,t)}{\partial x} = -\sigma N(x,t)\phi(x,t)$ and $\frac{\partial N(x,t)}{\partial t} = -\sigma N(x,t)\phi(x,t)$,

we will obtain:

$\phi(x,t) = \phi_0 \exp\big(-\sigma \mathrm{N}(x,t)\big)$

and $N(x,t) = N_0 \exp\big(-\sigma\xi(x,t)\big)$,

where ξ(x,t) is the neutron flux integrated over time or neutron fluence and N(x,t) is the nuclide density integrated over space, which are defined as follows, respectively: $\xi(x,t) \equiv \int_0^t dt'\phi(x,t')$ and $\mathrm{N}(x,t) \equiv \int_0^t dx' N(x',t)$.

Since equations $\phi(x,t) = \phi_0 \exp\big(-\sigma \mathrm{N}(x,t)\big)$ and $N(x,t) = N_0 \exp\big(-\sigma\xi(x,t)\big)$ are coupled and the solution of one depends on the solution of the other, we first obtain the asymptotic solution of equations $\frac{\partial\phi(x,t)}{\partial x} = -\sigma N(x,t)\phi(x,t)$ and $\frac{\partial N(x,t)}{\partial t} = -\sigma N(x,t)\phi(x,t)$ for each of ϕ and N and then use equations $\phi(x,t) = \phi_0 \exp\big(-\sigma \mathrm{N}(x,t)\big)$ and $N(x,t) = N_0 \exp\big(-\sigma\xi(x,t)\big)$ to obtain their exact solution. By this method, we can achieve exact solutions for the solitary waves resulting from Equations 4 and 5:

$$\varphi(x,t) = \varphi_0\left(\frac{1+\exp(-\sigma N_0 vt)}{1+\exp\big(\sigma N_0(x-vt)\big)}\right) \quad (11)$$

$$N(x,t) = N_0\left(\frac{1+\exp(\sigma N_0 x)}{\exp(\sigma N_0 vt)+\exp(\sigma N_0 x)}\right) \quad (12)$$

$$R(x,t) = \sigma\, N(x,t)\, \varphi(x,t) \quad (13)$$

In this work, we investigate the nuclear burnup characteristics of soliton waves (SWs) for several isotopic NAs, including boron (^{10}B), cadmium (^{113}Cd), samarium (^{149}Sm), europium (^{151}Eu), hafnium (^{177}Hf) and gadolinium (^{157}Gd). The net incident neutron flux is assumed to be 10^{14} cm^{-2} s^{-1} with neutrons incident normally on the slab boundary at x = 0 (see Fig. 1).

Table 2. Characteristics of selected different NAs in diffusive medium [35].

	^{10}B	^{113}Cd	^{149}Sm	^{151}Eu	^{177}Hf	^{157}Gd
Cross-sections (barns)	3847	20767	41000	9180	377	224000
Burnup wave velocity(cm/day)	0.83	4.55	8.80	2.0	0.09	54
Diffusion length (cm)	4.6	4.6	4.6	4.6	4.6	4.6
Number density (neutron/cm^3)	1.04×10^{19}	19×10^{17}	9.8×10^{17}	44×10^{17}	11×10^{19}	1.58×10^{17}

6. Results and Discussion

Using our suggested model, we plotted the two and three-dimensional NF, reaction rate, and nuclide density diagrams versus time and position in D_2O diffusive medium for each of the selected NAs, respectively. (See Figs. 2-4).

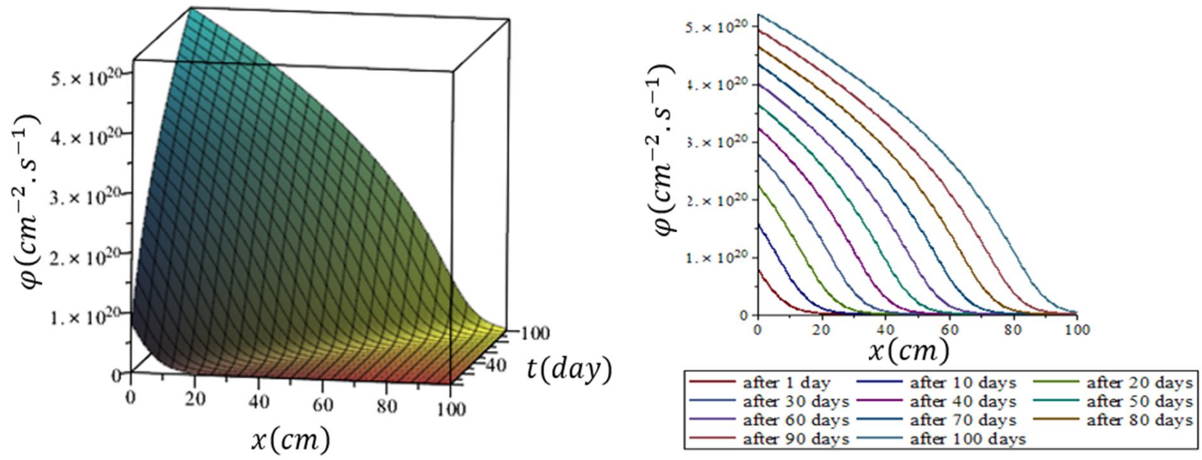
$\varphi(cm^{-2}.s^{-1})$
$x(cm)$
$t(day)$
after 1 day
after 10 days
after 20 days
after 30 days
after 40 days
after 50 days
after 60 days
after 70 days
after 80 days
after 90 days
after 100 days

A)

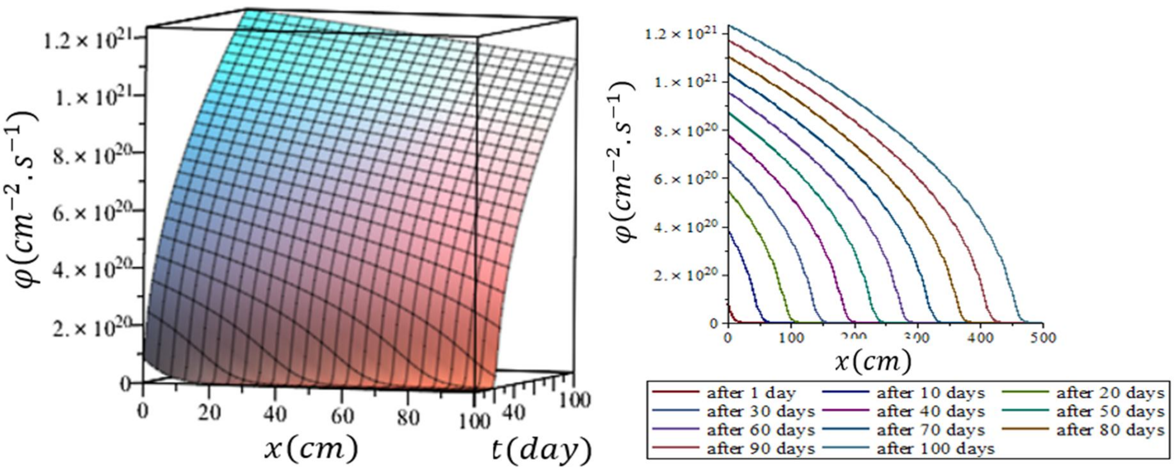
$\varphi(cm^{-2}.s^{-1})$
$x(cm)$
$t(day)$
after 1 day
after 10 days
after 20 days
after 30 days
after 40 days
after 50 days
after 60 days
after 70 days
after 80 days
after 90 days
after 100 days

B)

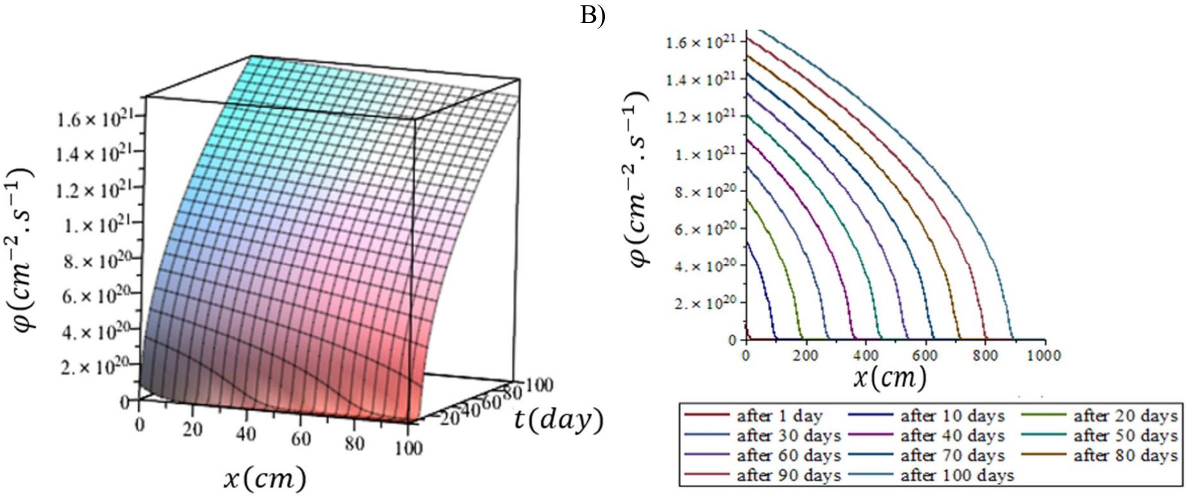
$\varphi(cm^{-2}.s^{-1})$
$x(cm)$
$t(day)$
after 1 day
after 10 days
after 20 days
after 30 days
after 40 days
after 50 days
after 60 days
after 70 days
after 80 days
after 90 days
after 100 days

C)

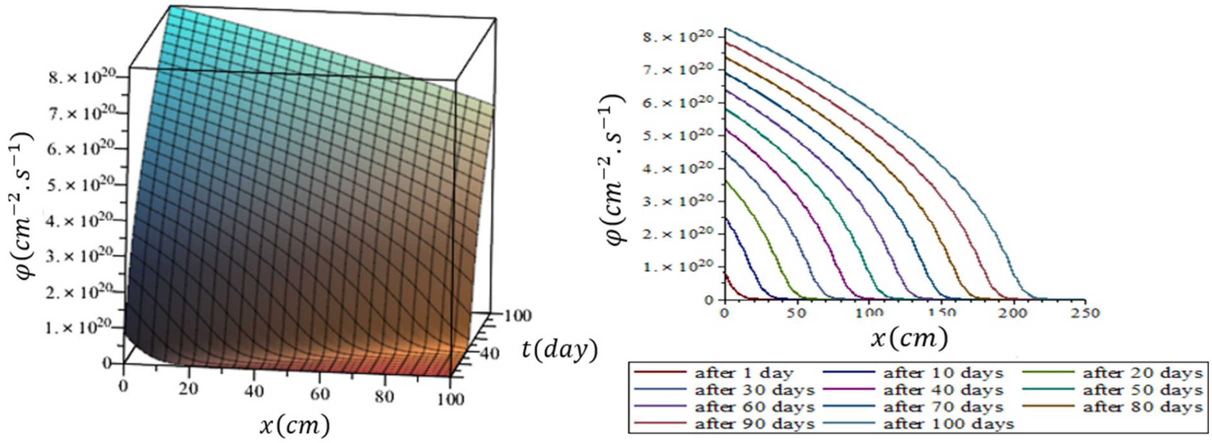

D)

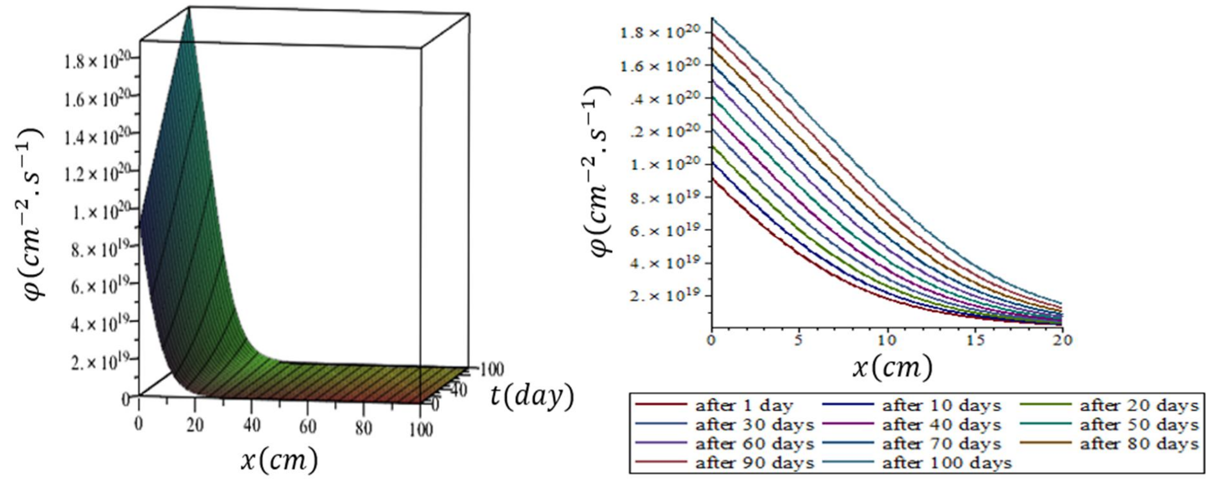

E)

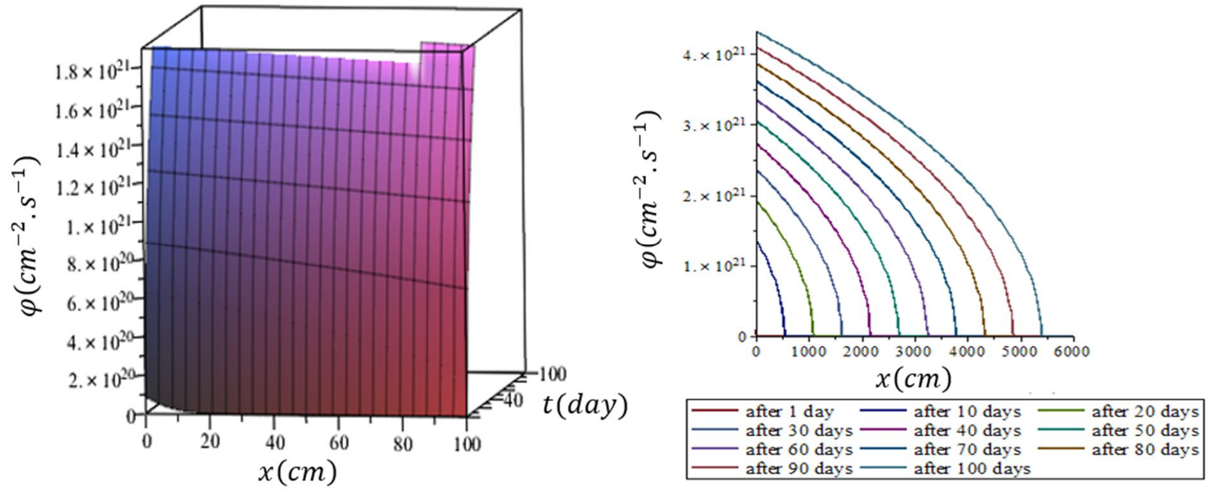

F)

FIG. 2. Two- and three-dimensional variations of φ for different neutron-absorbing media: A) Boron (^{10}B), B) Cadmium (^{113}Cd), C) Samarium (^{149}Sm), D) Europium (^{151}Eu), E) Hafnium (^{177}Hf), and F) Gadolinium (^{157}Gd)) versus position and time.

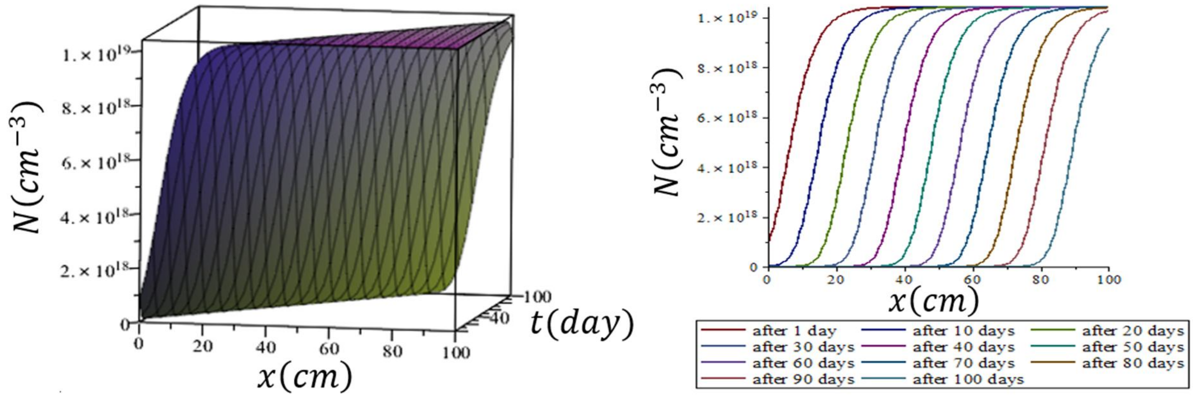
$N(cm^{-3})$
$t(day)$
$x(cm)$
after 1 day
after 10 days
after 20 days
after 30 days
after 40 days
after 50 days
after 60 days
after 70 days
after 80 days
after 90 days
after 100 days

A)

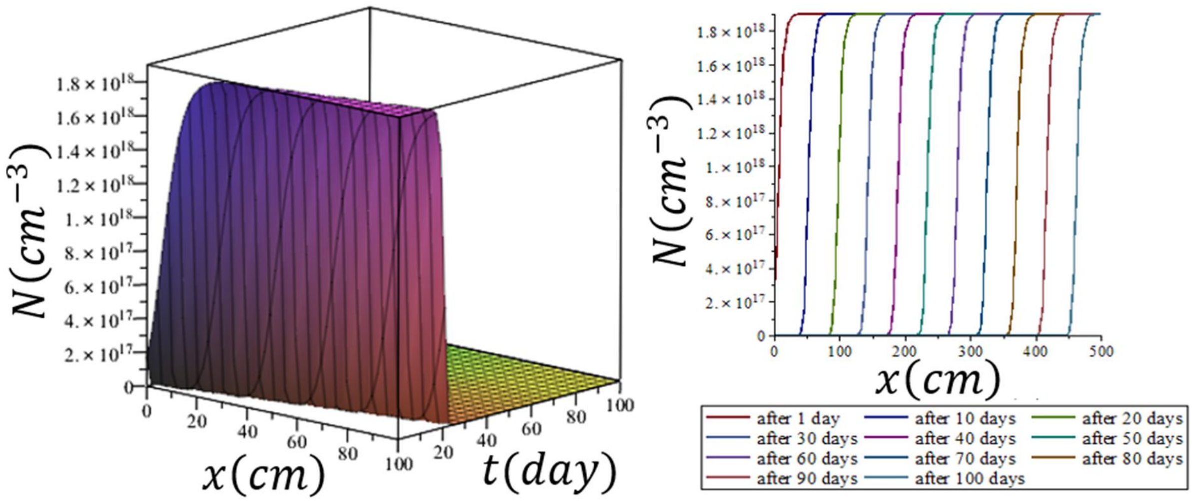
$N(cm^{-3})$
$t(day)$
$x(cm)$
after 1 day
after 10 days
after 20 days
after 30 days
after 40 days
after 50 days
after 60 days
after 70 days
after 80 days
after 90 days
after 100 days

B)

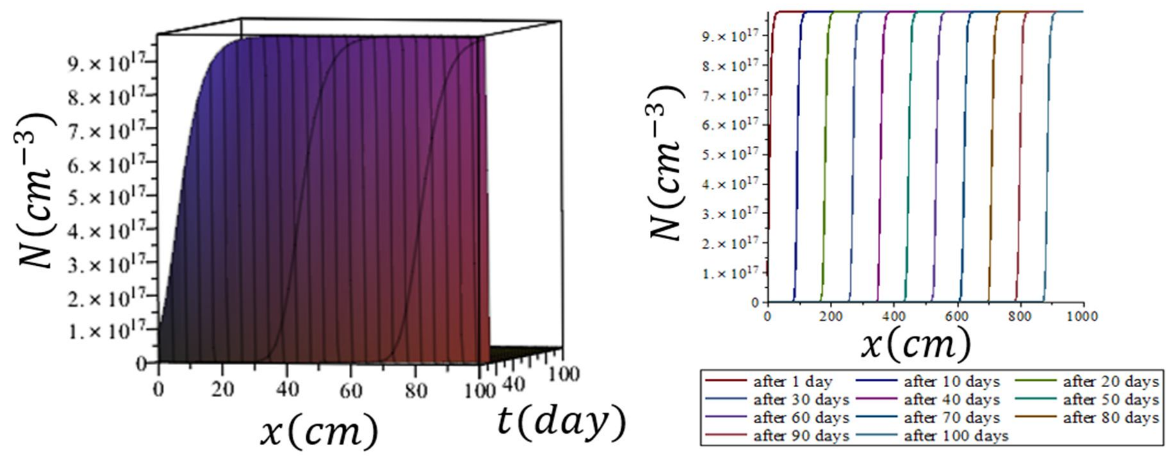
$N(cm^{-3})$
$t(day)$
$x(cm)$
after 1 day
after 10 days
after 20 days
after 30 days
after 40 days
after 50 days
after 60 days
after 70 days
after 80 days
after 90 days
after 100 days

C)

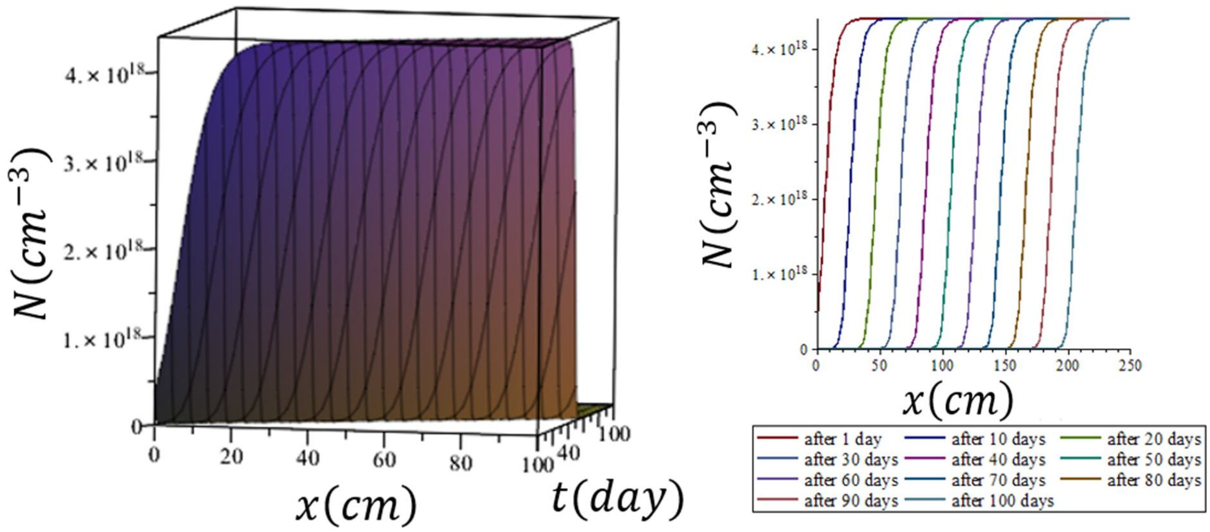

D)

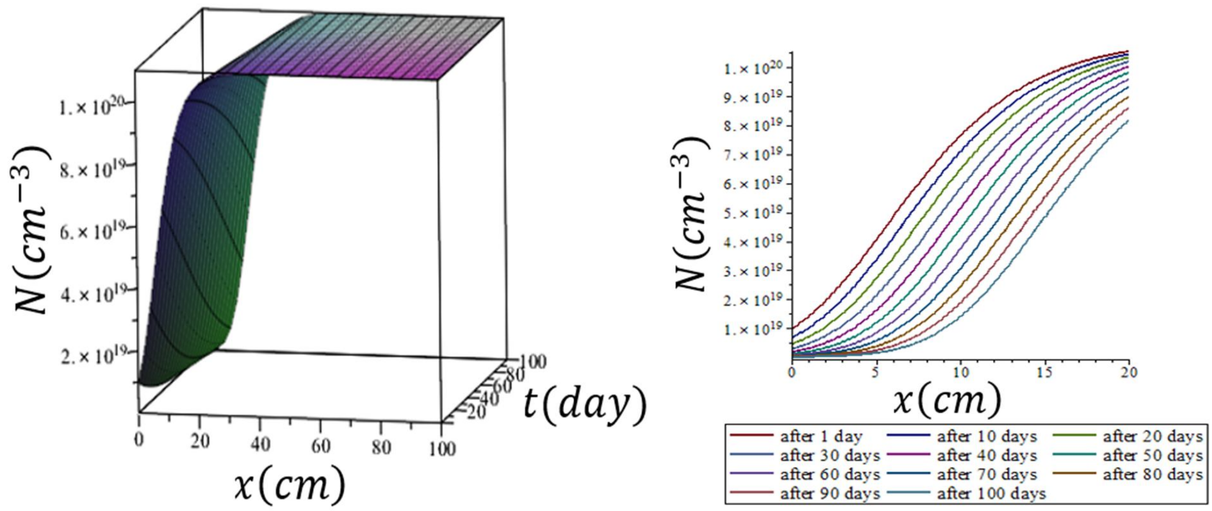

E)

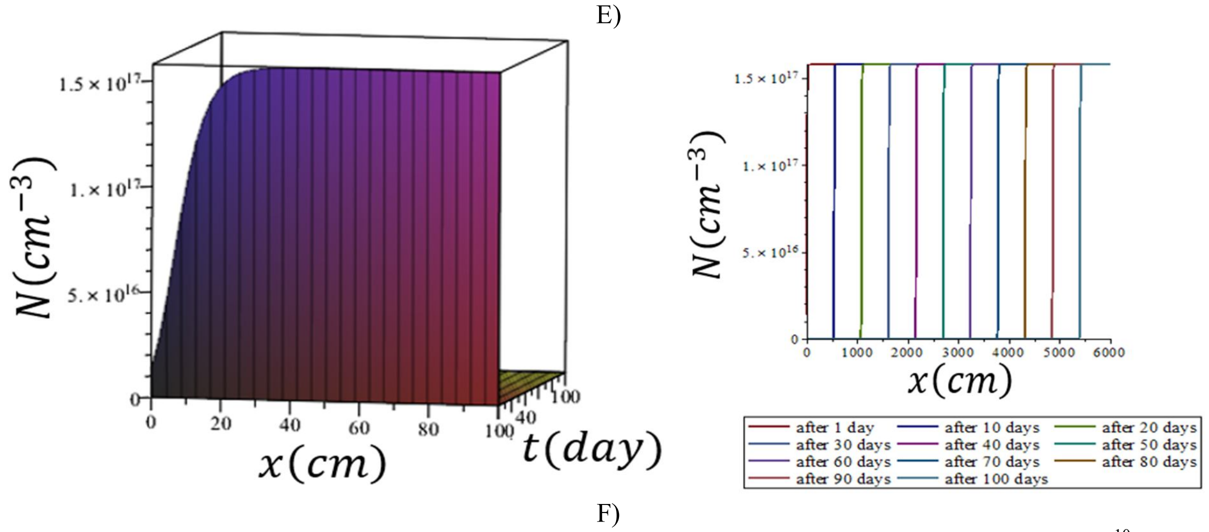

F)

FIG. 3. Two- and three-dimensional variations of N for different neutron-absorbing media: A) Boron (^{10}B), B) Cadmium (^{113}Cd), C) Samarium (^{149}Sm), D) Europium (^{151}Eu), E) Hafnium (^{177}Hf), and F) Gadolinium (^{157}Gd)) as functions of position and time.

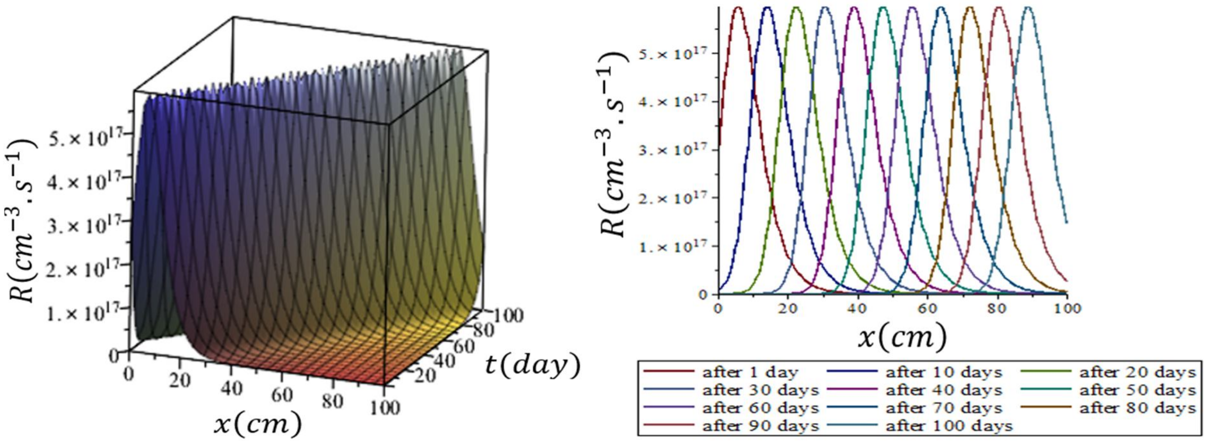
$R(cm^{-3}.s^{-1})$
$x(cm)$
$t(day)$
after 1 day
after 10 days
after 20 days
after 30 days
after 40 days
after 50 days
after 60 days
after 70 days
after 80 days
after 90 days
after 100 days

A)

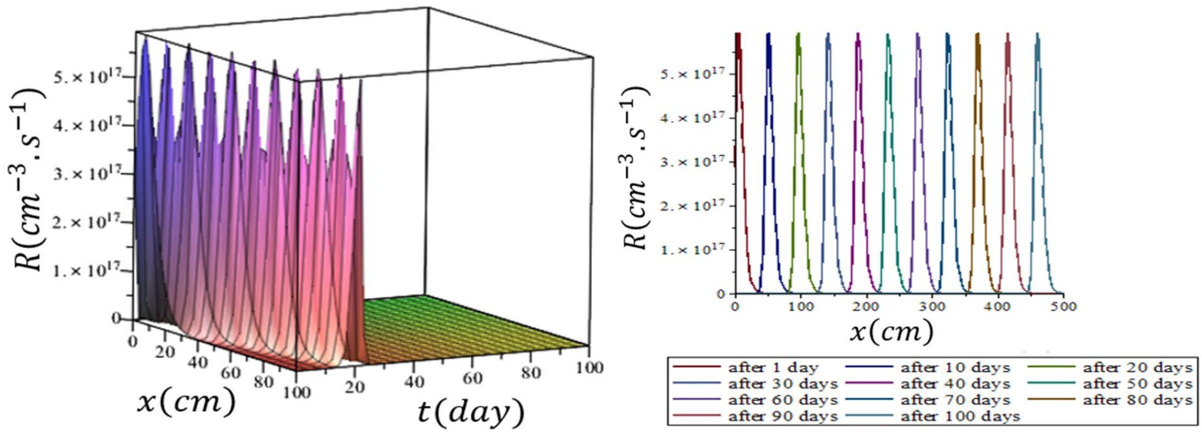
$R(cm^{-3}.s^{-1})$
$x(cm)$
$t(day)$
after 1 day
after 10 days
after 20 days
after 30 days
after 40 days
after 50 days
after 60 days
after 70 days
after 80 days
after 90 days
after 100 days

B)

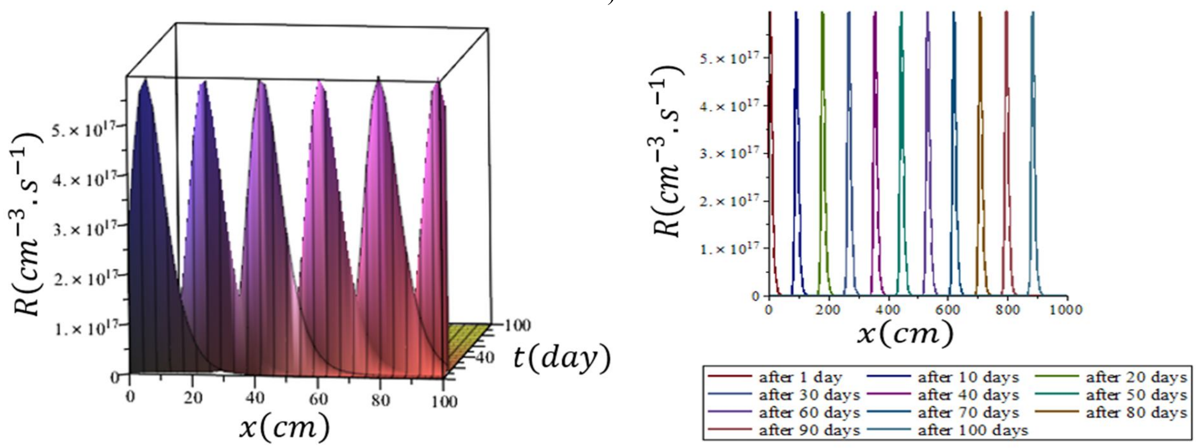
$R(cm^{-3}.s^{-1})$
$x(cm)$
$t(day)$
after 1 day
after 10 days
after 20 days
after 30 days
after 40 days
after 50 days
after 60 days
after 70 days
after 80 days
after 90 days
after 100 days

C)

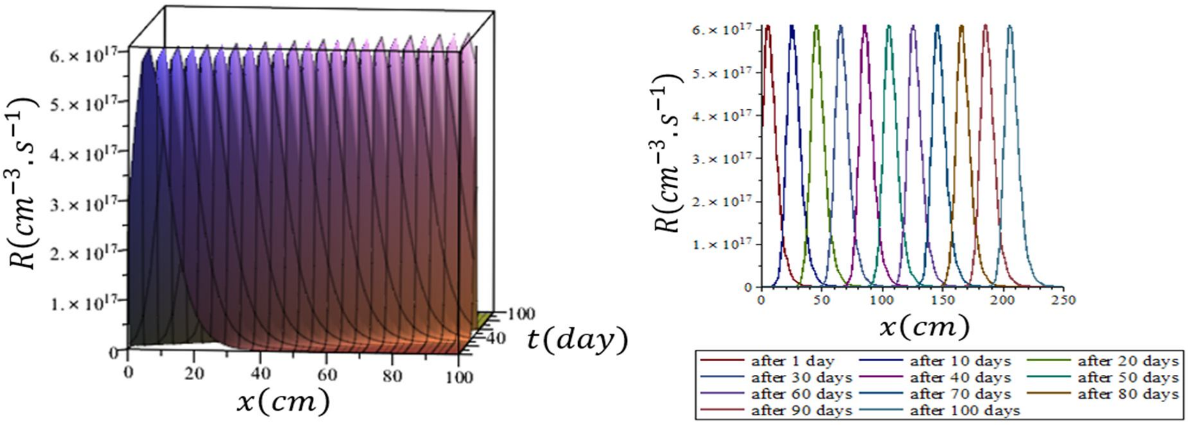

D)

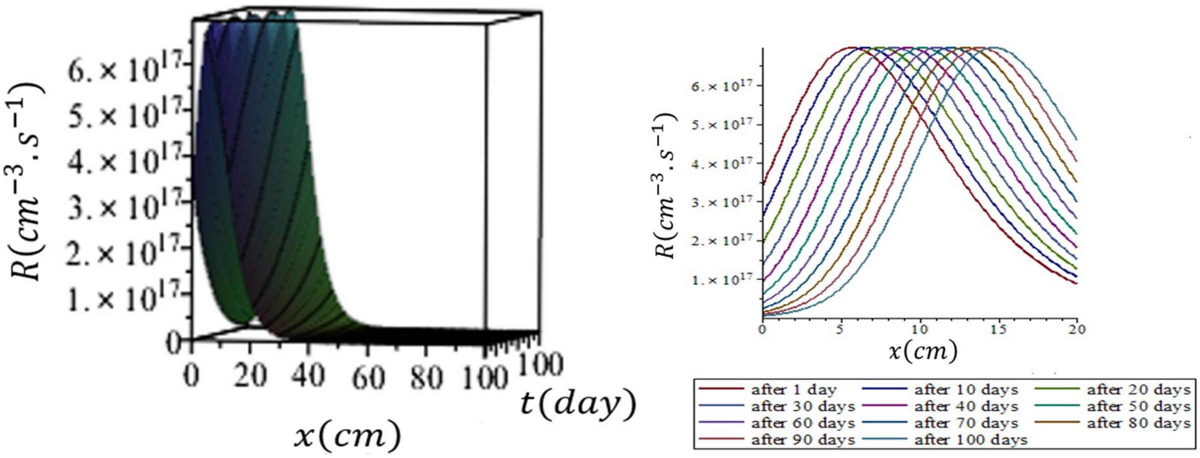

E)

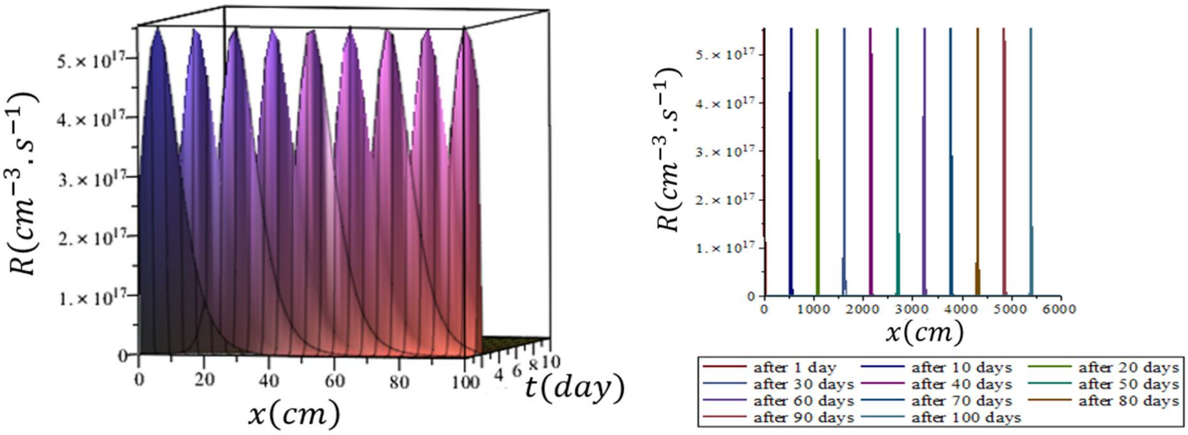

F)

FIG. 4. Two- and three-dimensional variations of R for different neutron-absorbing media: A) Boron (^{10}B), B) Cadmium (^{113}Cd), C) Samarium (^{149}Sm), D) Europium (^{151}Eu), E) Hafnium (^{177}Hf), and F) Gadolinium (^{157}Gd)) as functions of position and time.

The profiles of neutron flux, neutron fluence, and fuel density shown in Figs. 2-4 are obtained from the analytical solutions. Figure 2 demonstrates that the neutron flux exhibits a soliton-wave profile, whose amplitude decreases with increasing penetration depth and elapsed time. The evolution trends of the fuel density are also in good agreement with previous studies [35].

It is assumed that the diffusive medium is D_2O and no neutrons are absorbed through this medium. In order to simplify the matter under discussion, a geometrical shape of our system is considered as a finite slab. (see Fig. 1). Our numerical calculations show that, as neutrons penetrate deeper into the medium, the primary nuclides of the absorbing material are gradually consumed, resulting in a decrease in the density of the neutron-absorbing nuclides. This depletion process intensifies over time and continues throughout the burnup process. The transition time depends on the absorption cross section, σ_a; specifically as σ_a decreases، the transition time increases.

A detailed study has been carried out on the formation and characterization of nuclear burn-up waves in fast neutron multiplying media, with particular emphasis on the transient stage of the burnup wave. The transient characteristics are described using two parameters: the length of transient (LOT) and the time of transient (TOT), which represent the spatial length and elapsed time required to establish the asymptotic burnup wave, respectively. More specifically, the TOT and LOT are defined as the time and distance required to reach 95% and 99% of the asymptotic neutron flux propagating through the medium.

Using these parameters, the transient wave velocity is determined. The asymptotic characteristics of the wave are further evaluated in terms of the wave propagation velocity and the Full Width at Half Maximum (FWHM) of the neutron flux spatial distribution. The diffusion equations were solved and the figures were generated using Maple 20 software.

Our numerical calculations show that hafnium has the longest TOT among the materials considered in this study, which is consistent with results reported for graphite diffusive medium [35]. In contrast, hafnium possesses the minimum value of LOT. This indicates that, despite its relatively short transient length, hafnium requires a longer time to reach the steady-state condition compared with other materials.

From the plotted diagrams in Fig. 4, we find that the reaction-rate distribution rapidly approaches the asymptotic form given in Eq. (9). The TOT values corresponding to cadmium, samarium, europium, boron and gadolinium neutron absorbers are smaller than that of hafnium. Therefore, a longer time interval of 10 days was considered when plotting the hafnium results.

From these figures, the characteristic properties of the solitary burnup wave for the selected absorbers in a D_2O diffusive medium were calculated and are summarized in Table 3.

These figures are characterized by the time of transient (TOT), the length of transient (LOT), and the steady-state (SS) phase parameters which are described as follows:

a) Time of transient (TOT) represents the time required for the burnup wave to reach its asymptotic form. In other words, it corresponds to the duration of the transient phase. Typically, the TOT varies rapidly during the initial stage and then changes more gradually as the system approaches the steady state.

b) Length of transient (LOT) represents the spatial distance traveled by the wave before reaching the steady-state condition.

c) Steady-state (SS) phase includes two basic parameters:

(1) Wave velocity is estimated from the ratio of the net incedent neutron current to the initial nuclide density.

(2) Width of the reaction rate region is quantified using the Full Width at Half Maximum (FWHM).

It should be noted that, for each diffusive medium, the characteristic time and diffusion length differ because of variations in material abundance and absorption cross section, σ_a. The values of these quantities are listed in Table 3. Accordingly, the numerical values of TOT and LOT can be analyzed in relation to the characteristic time and diffusion length.

The following results are obtained from Table 3:

1. The calculated propagation speed of the burnup wave is independent of the diffusion coefficient, in agreement with the theoretical prediction.
2. As the diffusion coefficient increases, the LOT also increases. However, the ratio of the LOT to the diffusion length does not change.
3. The TOT increases with increasing diffusion coefficient.
4. The FWHM of the burnup SW increases as the diffusion coefficient increases.

In this work, analytical solutions for an advanced nuclear power system, namely the traveling wave reactor (TWR), are presented by coupling the one-dimensional neutron diffusion equation with the burnup equation. To obtain tractable analytical solutions, several necessary simplifications are adopted. Analytical expressions for the neutron flux, neutron current, and nuclide density evolution are derived and represented in the form of solitary waves. Appropriate parameters are then selected to apply and verify the analytical solutions. The results indicate that the neutron flux is directly proportional to the wave velocity and inversely proportional to both the fuel density and the microscopic absorption cross section. The neutron flux exhibits a bell-shaped solitary-wave profile, whose characteristics are influences by the wave velocity, fuel density, and microscopic absorption cross section.

The calculations further show that the maximum neutron flux is independent of the wave velocity and primarily depends on the properties of the neutron-absorbing medium. These analytical solutions provide valuable physical insight into the behavior of advanced nuclear power systems. Nevertheless, future studies should extend the present analysis to multidimensional analytical solutions in order to broaden the scope of the investigation.

Table 3. Characteristics of the calculated neutron burnup soliton waves (SWs) for different selected neutron absorbers (NAs) in a D_2O diffusive medium.

Isotopic neutron absorbers	^{10}B	^{113}Cd	^{149}Sm	^{151}Eu	^{177}Hf	^{157}Gd
Initial absorber density (atoms/Cm^3)	1.04×10^{19}	19×10^{17}	9.8×10^{17}	44×10^{17}	11×10^{19}	1.58×10^{17}
Cross-sections (barns)	3847	20767	41000	9180	377	224000
Velocity simulation (cm/day)	0.83	4.6	8.8	2	0.08	55
Velocity analytical (cm/day)	0.80	4.5	8.8	2.0	0.1	54.7
LOT (Cm)	13.8	13.9	13.8	13.8	13.6	13.7
Diffusion length (cm)	4.6	4.6	4.6	4.6	4.6	4.6
LOT /Diffusion length	3	3	3	3	3	3
TOT (days)	16.6	3.1	1.6	7.0	172.9	0.3
Characteristics time, τ(days)	5.55	1.02	0.52	2.34	57.64	0.09
TOT / characteristics time	3.1	3.1	3.1	3.1	3.1	3.1
FWHM (cm)	13.0	13.0	12.9	12.9	12.7	13.8
FWHM/ diffusion length	2.81	2.81	2.81	2.81	2.81	2.81

7. Conclusion

In this research, we investigate the behavior of solitary waves (SWs) in a uniform medium consisting of different neutron-absorbing materials and a heavy-water diffusive medium. This study contributes to the understanding of burnup SW propagation in diffusive media containing different NAs and provides a description of the fundamental properties of solitons.

To achieve this objective, the reactor geometry is modeled as a finite one-dimensional slab. Owing to its simplicity, the one-dimensional slab geometry is particularly suitable for analyzing the behavior of SWs and deriving analytical solutions. In the one-dimensional case, the model is solved analytically. The solitary-wave solution, referred to as the fundamental solution of the coupled burnup-diffusion system, is derived, and the conditions required for its existence are discussed.

For a purely absorbing medium, neutron scattering by nuclides is assumed to be neglible. If an increase in the burnup SW propagation speed is required, the density of the absorbing material must be reduced by introducing materials with low neutron absorption capability. Heavy water is considered as the diffusive medium in this work.

Our study investigates six NA media: boron carbide, cadmium, samarium, europium, hafnium and gadolinium. It should be noted that the initial incident neutron flux is assumed to be identical for all cases and equal to 10^{14} cm^{-2} s^{-1}. Our numerical calculations show that the propagation speed of the burnup wave remains unchanged with increasing diffusion coefficient. However, both the diffusion length and the LOT increase. Furthermore, the ratio between the LOT and diffusion length remains constant. Similarly, increasing the diffusion coefficient leads to an increase in the TOT, while the ratio between the TOT and the characteristic time remains constant.

This research introduces new parameters and methods for describing SW propagation and its relationship with the inherent parameters of the reactor system. In particular, it establishes relationships between the LOT, TOT, and wave velocity with important reactor parameters such as the absorption cross section, mean free path, and characteristic time.

The following suggestions are proposed for future research:

1. Extending and generalizing the present analysis to additional neutron-absorbing elements and reactor media.
2. Investigating the selected materials by considering not only the proposed wave parameters but also economic factors and the chemical and physical properties relevant to their application in research nuclear reactors.
3. Applying the proposed parameters to support the design and optimization of nuclear fuel systems and the practical implementation of burnup SW concepts.

References

[1] Russell, J.S., Report on Waves: 14th Meeting of the British Association for the Advancement of Science, John Murray, London, 311 (1844).

[2] Iwata, Y. and Stevenson, P., New Journal of Physics, 21 (2019) 043010.

[3] Sekizawa, K., Frontiers in Physics, 7 (2019) 20.

[4] Simenel, C. and Umar, A.S., Progress in Particle and Nuclear Physics, 103 (2018) 19.

[5] Stevenson, P. and Barton, M.C., Progress in Particle and Nuclear Physics, 104 (2019) 142.

[6] Wazwaz, A.M. and Peakons, K., Applied Mathematics and Computation, 182 (2006) 412.

[7] Zabusky, N.J. and Kruskal. M.D., Physical Review Letters, 15 (1965) 240.

[8] Seifritz, W., Kerntechnik, 60 (1995) 185.

[9] Van Dam Hugo, H., Annals of Nuclear Energy, 25 (1998) 1409.

[10] Van Dam, H, Annals of Nuclear Energy, 27 (2000a) 63.

[11] Van Dam, H., Annals of Nuclear Energy, 27 (2000b) 733.

[12] Huang, J.F., Nuclear Science and Engineering, 196 (2022) 213.

[9] Anoop, K.V. and Pal Singh, O.M., Sådhanå, 43 (2018) 11.

[13] Duderstadt, J.J. and Hamilton, L.J., "Nuclear Reactor Analysis", (Wiley, New York, 1976).

[14] Frenkel, J. and Kontrova, T., Journal of Physics USSR, 1 (1939) 137.

[15] Skyrme, T.H.R., Proceedings of the Royal Society A, 247 (1958) 260.

[16] Hasegawa, A. and Tappert, F., Applied Physics Letters, 23 (1973) 171.

[17] Huang, J. et al., Progress in Nuclear Energy, 85 (2015) 11.

[18] Kaplan, M., Akbulut, A., and Al Qahtani, R.T., Mathematics, 11 (2023) 181.

[19] Alotaibi, M.F., Raza, N., Rafiq, M.H., and Soltani, A., Alexandria Engineering Journal, 67 (2023) 583.

[20] Tarla, S., Ali, K.K., Sun, T.C., Yilmazer, R., and Osman, M.S., Results in Physics, 36 (2022) 105381.

[21] Wang, K.J., Liu, J.H., and Wu, J., Optik Journal, 251 (2022) 168319.

[22] Rao, J., He, J., and Mihalache, D., Applied Mathematics Letters, 121 (2021) 107435.

[23] Tongpeng, S., Makbun, K., Peanporm, P., Sangkorn, R., Namsar, O., Janphuang, P., Pojprapai, S., and Jainsirisomboon, S., Materials Today: Proceedings, 17 (2019) 1555.

[24] Zeman, M., Skoda, R., and Zavorka, J., Proceedings of the 26th International Conference on Nuclear Engineering, Vol. 9, (2018).

[25] Abu Sondos, M.A., Jordan Journal of Physics, 16 (1) (2023) 91.

[26] Dandi, A., Lee, M., and Kim, M.H., Nuclear Engineering and Technology, 52 (2) (2020) 238.

[27] Guo, H., Kooyman, T., Sciora, P., and Buiron, L., Nuclear Technology, 205 (11) (2019) 1447.

[28] Tonks, M., Andersson, D., Devanathan, R., Dubourg, R., El-Azab, A., Freyss, M., Iglesias, F., Kulacsy, K., Pastore, G., Phillpot, S.R., and Welland, M., Journal of Nuclear Materials, 504 (2018) 300.

[29] Campolina, D., Faria, E.F., Santos, A.A.C., Vasconcelos, V., Franco, M.P.V., Dias, M.S., and Mattos, J.R.L., Annals of Nuclear Energy, 118 (2018) 375.

[30] Papynov, E.K., Shichalin, O.O., Mironenko, A.Y., Tananaev, I.G., Avramenko, V.A., and Sergienko, V.I., International Conference on Mechanical Engineering and Applied Composite Materials, 307 (2018).

[31] Balice, L., Cologna, M., Audubert, F., and Hazemann, J.-L., Journal of the European Ceramic Society, 41 (1) (2021) 719.

[32] Papynov, E.K., Shichalin, O.O., Belov, A.A., Portnyagin, A.S., Buravlev, I.Y., Mayorov, V.Y., Sukhorada, A.E., Gridasova, E.A., Nomerovskiy, A.D., Glavinskaya, V.O., Tananaev, I.G., and Sergienko, V.I., Nuclear Engineering and Technology, 52 (8) (2020) 1756.

[33] Kardoulaki, E., White, J.T., Byler, D.D., Frazer, D.M., Shivprasad, A.P., Saleh, T.A., Gong, B., Yao, T., Lian, J., and Mcclellan, K.J., Journal of Alloys and Compounds, 818 (25) (2020) 153216.

[34] Guo, H., Buiron, L., Sciora, P., and Kooyman, T., Nuclear Engineering and Technology, 52 (7) (2020) 1367.

[35] Guo, H., Sciora, P., Kooyman, T., Buiron, L., and Rimpault, G., Nuclear Technology, 205 (11) (2019) 1433.

[36] Hosseinimotlagh, S.N. et al., Kerntechnik, 89 (2024) 5.

[37] Wang, K.J., Optik, 249 (2022) 168265.

[38] Kalcheva, S. and Branden, G.V.D., International Conference on Mathematics & Computational Methods Applied to Nuclear Science & Engineering, Korean Nuclear Society, Jeju, Korea, (2017).

[39] Franck, N., Kalcheva, S., and Koonen, E., Proceedings of the 13th International Topical Meeting on Research Reactor Fuel Management، Vienna, Austria, (2009).

[40] Kalcheva, S., Branden, G.V.D., and Koonen, E., Prague, Czech Republic, (2012).

[41] Anoop, K.V., Kiran, B., and Singh, O.P., Applied Mathematics and Mechanics, 7 (2015) 47.